Cover Page

Manuscript type: New Methods and Materials

Virtual indigo carmine chromoendoscopy images: A novel modality for peroral cholangioscopy using artificial intelligence technology (with video)

Authors: Ryosuke Sato, MD[1]; Kazuyuki Matsumoto, MD, PhD[1]; Hideaki Kinugasa, MD, PhD[1]; Masahiro Tomiya, BS[2], Takayoshi Tanimoto, BS[2], Akimitsu Ohto, BS[2], Kei Harada, MD[1]; Nao Hattori, MD[1]; Taisuke Obata, MD[1]; Akihiro Matsumi, MD, PhD[1]; Kazuya Miyamoto, MD, PhD[1]; Kosaku Morimoto, MD[1]; Hiroyuki Terasawa, MD, PhD[1]; Yuki Fujii, MD, PhD[1]; Daisuke Uchida, MD, PhD[1]; Koichiro Tsutsumi, MD, PhD[1]; Shigeru Horiguchi, MD, PhD[1]; Hironari Kato, MD, PhD[1]; Yoshiro Kawahara, MD, PhD[1]; and Motoyuki Otsuka, MD, PhD[1]

Institution: [1] Department of Gastroenterology and Hepatology, Okayama University Hospital, Okayama, Japan

[2] Business Strategy Division, Ryobi Systems Co., Ltd., Okayama, Japan

Corresponding author: Kazuyuki Matsumoto, M.D. PhD.

Department of Gastroenterology and Hepatology, Okayama University Hospital, 2-5-1 Shikata-cho, Kita-ku, Okayama-city, Okayama, 700-8558, Japan.

E-mail: matsumoto.k@okayama-u.ac.jp

Fax: +81-86-225-5991

Phone: +81-86-235-7219

Trial registry number: This study was approved by the Institutional Review Board of Okayama University Hospital (2203-017).

Guarantor of the article: Kazuyuki Matsumoto, M.D. PhD.

Specific author contributions: R.S. and K.M. conceived and designed the study and wrote the manuscript. K.H. and H.K. advised on the concept of the paper. Y.K. and M.T. provided information on artificial intelligence. T.T. and A.O. provided technical assistance. K.H. and N.H. collected endoscopic images. T.O. and A.M. collected references on previous studies. K.M. and K.M. reviewed the methods. H.T. and Y.F. reviewed the figures and tables. D.U. and K.T. assisted with proofreading. S.H. critically revised the article for important intellectual content. M.O. approved the study. All the authors have read and approved the final version of this manuscript.

Financial support: None to report.

Competing interests: The authors declare that they have no conflict of interest.

Acknowledgements: Not applicable.

Graphical abstract

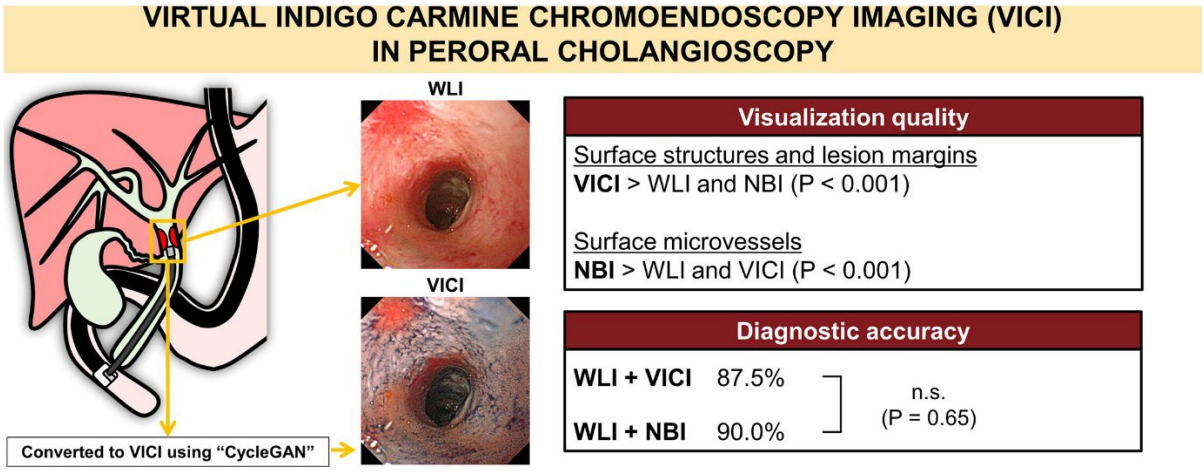

Abstract

Background and Aims: Accurately diagnosing biliary strictures is crucial for surgical decisions, and although peroral cholangioscopy (POCS) aids in visual diagnosis, diagnosing malignancies or determining lesion margins via this route remains challenging. Indigo carmine is commonly used to evaluate lesions during gastrointestinal endoscopy. We aimed to establish the utility of virtual indigo carmine chromoendoscopy (VICI) converted from POCS images using artificial intelligence.

Methods: This single-center, retrospective study analyzed 40 patients with biliary strictures who underwent POCS using white light imaging (WLI) and narrow-band imaging (NBI). A "cycle-consistent adversarial network" (CycleGAN) was used to convert the WLI into VICI of POCS images. Three experienced endoscopists evaluated WLI, NBI, and VICI via POCS in all patients. The primary outcome was the visualization quality of surface structures, surface microvessels, and lesion margins. The secondary outcome was diagnostic accuracy.

Results: VICI showed superior visualization of the surface structures and lesion margins compared with WLI ($P<0.001$) and NBI ($P<0.001$). The diagnostic accuracies were 72.5%, 87.5%, and 90.0% in WLI alone, WLI and VICI simultaneously, and WLI and NBI simultaneously, respectively. WLI and VICI simultaneously tended to result in higher accuracy than WLI alone ($P=0.083$) and the results were not significantly different from WLI and NBI simultaneously ($P=0.65$).

Conclusions: VICI in POCS proved valuable for visualizing surface structures and lesion margins and contributed to higher diagnostic accuracy comparable to NBI. In addition to NBI, VICI may be a novel supportive modality for POCS.

Keywords: cycle-consistent adversarial network; peroral cholangioscopy; virtual indigo carmine chromoendoscopy

INTRODUCTION

Accurately diagnosing benign or malignant conditions and recognizing lesion margins in patients with indeterminate biliary strictures are required to determine the surgical indication, surgical procedure, and prognosis. Peroral cholangioscopy (POCS) is frequently employed to visualize biliary strictures, offering the advantages of visualization-guided biopsy and improved diagnostic accuracy compared to fluoroscopic biopsy[1]. Preoperative confirmation of the extent of the lesions is essential as bile duct cancer often involves the superficial layers of the bile duct mucosa, thereby influencing the choice of surgical procedure. Therefore, preoperative POCS is critical in patients with biliary strictures. Detailed observation of the bile duct mucosa is achievable during POCS using white light imaging (WLI) and narrow-band imaging (NBI), facilitating high-precision diagnostics based on the classification of POCS findings, with particular attention to surface structures and microvessels for bile duct neoplasms[2]. However, diagnosing malignancy or determining lesion margins using conventional imaging alone remains challenging.

In gastrointestinal endoscopy, image-enhanced endoscopy including NBI and chromoendoscopy using stains or dyes is widely used to differentiate between benign and malignant lesions and to diagnose the extent of lesions[3,4]. Chromoendoscopy with sprayed indigo carmine is an important modality comparable to WLI and NBI and is commonly performed to improve the visibility of mucosal abnormalities and visualize the extent of lesions via gastrointestinal endoscopy[5]. Bile duct cancer generally arises from the mucosa of the bile duct; therefore, the visibility of mucosal abnormalities in POCS is expected to contribute to the diagnosis of the extent and determine whether it is benign or malignant. However, due to the presence of bile or saline in the bile duct lumen during POCS, indigo carmine spraying is challenging.

In a previous study, we successfully converted POCS images to virtual indigo carmine

chromoendoscopy imaging (VICI) using one of the artificial intelligence technologies, "cycle-consistent adversarial network" (CycleGAN), which enables image transformation[6]. Using indigo carmine-sprayed images from gastrointestinal endoscopy as training data, this technology enables virtual chromoendoscopy without spraying indigo carmine into the bile duct. In this study, we evaluated the diagnostic utility of VICI in POCS compared to that of WLI and NBI.

METHODS

Patients

A total of 114 patients with indeterminate biliary strictures who underwent POCS between January 2012 and October 2023 were retrospectively enrolled. Patients over 20 years of age with hilar bile duct or distal bile duct stenosis, who underwent endoscopic sphincterotomies (ESTs) or papillary balloon dilations prior to POCS insertion, and those with a bile duct diameter (> 8 mm) sufficient for POCS insertion were included. Among them, 33 patients who underwent POCS with SpyScope™ DS or SpyScope™ DSII (Boston Scientific, Massachusetts, USA), on which NBI was not available, 37 patients without NBI, and 4 patients without technical success were excluded. Finally, 40 patients in whom biliary strictures were observed on POCS using both WLI and NBI and histopathological evaluations were possible using biopsy or surgical specimens were included. This study was approved by the Institutional Review Board of Okayama University Hospital (2203-017).

Peroral cholangioscopy procedure

All patients underwent endoscopic retrograde cholangiopancreatography (ERCP) and POCS in the prone position under conscious sedation with intravenous diazepam and pethidine hydrochloride. POCS was performed using a duodenoscope (TJF-240, TJF-260V, or TJF-

Q290V; Olympus Medical, Tokyo, Japan) immediately after stricture evaluation using ERCP or a few days after endoscopic nasobiliary drainage (ENBD) tube insertion. EST or papillary balloon dilation was performed in all patients. After ERCP completion, prophylactic antibiotics were administered intravenously, and a protease inhibitor was administered to prevent pancreatitis. During POCS, CHF-B260 was used until 2019 and CHF-B290 (Olympus Medical, Tokyo, Japan), which provides a wider field of view that ranges from 1.5 mm to as far as 20 mm, enhancing near-point image quality, was used from 2020. Both scopes were used via the mother-baby method by two endoscopists who had performed more than 500 ERCPs, with one endoscopist operating the duodenoscope and the other using cholangioscopy. After insertion of the cholangioscope into the bile duct, bile duct strictures were visualized by bile aspiration and irrigation with a saline solution. Ten to 30 cholangioscopic images of bile strictures were recorded using WLI, followed by 10–15 images using NBI. At least three POCS-guided forceps biopsies of the strictures were performed after cholangioscopic evaluation. Biliary drainage was performed after biopsy when needed. The final diagnoses were made based on the surgical specimen if surgeries were performed or biopsy specimens when biopsies showed malignant findings if surgeries were not performed. If the biopsies showed no malignant results, the patients were followed up with imaging and laboratory examinations for at least 6 months, and the strictures were diagnosed as benign.

Converting to virtual indigo carmine chromoendoscopy imaging

"CycleGAN" is an artificial intelligence technology that enables image-style transformation using unsupervised learning without paired images[7]. For example, in the field of gastrointestinal endoscopy, "CycleGAN" can be converted from WLI to VICI and from indigo carmine-sprayed images to pseudo-WLI by training two types of images, WLI and indigo carmine-sprayed images, as datasets[8]. In this study, we used "CycleGAN" to convert WLI to

VICI of POCS images by diverting training data of gastrointestinal endoscopic images (1,429 stomach images and 556 colon images of WLI, 790 stomach images and 106 colon images that were indigo carmine sprayed [Fig. 1]). The network was trained with a learning rate of 0.0002, 200 epochs, and a batch size of 1 (Video 1).

Outcome measurements

The primary outcome was the visualization quality of the surface structures, surface microvessels, and lesion margins using WLIs, NBIs, and VICIs in POCS. Three experienced biliopancreatic endoscopists blindly evaluated WLIs, NBIs, and VICIs for POCS in all patients without patient information. For training, 10 samples of VICIs in POCS were provided and observed (Supplementary Table 1). The surface structures, surface microvessels, and lesion margins were evaluated on a scale of "poor," "fair," or "excellent." For surface structures and surface microvessels, "poor" was defined as difficult to identify, "fair" as easy to observe but challenging to identify patterns, and "excellent" as easy to identify patterns, such as papillary or nodular for surface structures and dilated or tortuous for surface microvessels. For lesion margins, "poor" was defined as the lesion being difficult to distinguish from the normal area, "fair" as the lesion being recognizable as a region and the margin could be inferred, and "excellent" as the margin between the lesion and the normal area being clearly identifiable (Supplementary Fig. 1). In cases of disagreement, the endoscopists discussed the final results and performed a single evaluation of each imaging mode for each patient. The secondary outcome was the diagnostic accuracy. To verify the effect of VICI and NBI on the accuracy of benign and malignant diagnosis for WLI, the endoscopists read all cases in three patterns: WLI alone, WLI and VICI simultaneously, and WLI and NBI simultaneously, and made a diagnosis of whether benign or malignant lesions were present in each patient. The diagnostic accuracies of each pattern were also compared.

Statistical analysis

Categorical evaluation scales for WLI, NBI, and VICI of POCS were compared with those of other imaging modes using the Friedman test, followed by the Steel–Dwass test. The diagnostic ability was determined in terms of accuracy, sensitivity, and specificity for diagnosing malignancy with a 95% confidence interval (CI). McNemar's test was used to compare the additive diagnostic accuracies of VICI and NBI for WLI. Receiver operating characteristic (ROC) curves were calculated for the accuracies of WLI alone, WLI and VICI simultaneously, and WLI and NBI simultaneously, and the areas under the ROC curves (AUCs) were calculated from each ROC curve and compared. Statistical significance was set at $P<0.05$. JMP software version 17.0 was used to perform statistical calculations (SAS Institute, Cary, North Caronia, USA).

RESULTS

Patient flow and characteristics

A patient flow diagram is shown in Fig. 2. In the enrolled 40 patients who underwent POCS with both WLI and NBI, benign or malignant diagnoses were made using surgical specimens or POCS biopsies of biliary strictures. Of the 30 patients with malignancy, 21 underwent surgery, and 9 were diagnosed with unresectable disease and treated with chemotherapy or observation. Of the 10 patients diagnosed with benign lesions, 9 were followed up for more than 1 year to confirm the absence of malignant findings. Only one patient diagnosed with a benign lesion on biopsy could not be ruled out as malignant by imaging findings; this patient underwent surgery and was finally diagnosed with a benign disease (immunoglobulin G4-related sclerosing cholangitis; IgG4-SC). The characteristics of the 40 patients included a median age of 74 years (range, 47–89), 33 males, 30 malignant diseases (15 distal bile duct

cancers, 12 hilar bile duct cancers, 2 intrahepatic bile duct cancers, and 1 gallbladder cancer), and 10 benign diseases (5 secondary sclerosing cholangitis, 3 IgG4-SCs, 1 anastomotic stricture after living-donor liver transplantation, and 1 follicular cholangitis). During POCS, CHF-B290 and CHF-B260 were used in 21 and 19 cases, respectively. (Table 1).

Visualization quality

The three endoscopists provided one visualization rate for each imaging mode for all 40 cases (Fig. 3, Fig. 4, and Table 2). Regarding surface structures, 27 (67.5%) cases were evaluated as "fair," both on WLI and NBI, whereas 29 (72.5%) cases were evaluated as "excellent" on VICI. Regarding surface microvessels, 25 (62.5%) cases were evaluated as "fair" on WLI, and 33 (82.5%) cases were evaluated as "poor" on VICI, whereas 28 (70.0%) cases were evaluated as "excellent" on NBI. Regarding lesion margins, 34 (85.0%) and 22 (55.0%) cases were evaluated as "fair" on WLI and NBI, respectively, whereas 21 (52.5%) cases were evaluated as "excellent" on VICI. Regarding surface structures and lesion margins, VICI showed superior visualization compared to WLI (Steel–Dwass test: $P<0.001$) and NBI (Steel–Dwass test: $P<0.001$), whereas NBI showed superior visualization of surface microvessels compared to WLI (Steel–Dwass test: $P<0.001$) and VICI (Steel–Dwass test: $P<0.001$).

Diagnostic ability

The diagnosis by endoscopists showed that WLI alone had an accuracy of 72.5% (95% CI: 58.7–86.3), sensitivity of 76.7% (95% CI: 61.5–91.8), and specificity of 60.0% (95% CI: 29.6–90.4), respectively. WLI and VICI simultaneously had an accuracy of 87.5% (95% CI: 77.3–97.7), sensitivity of 90.0% (95% CI: 79.3–100.7), and specificity of 80.0% (55.2–104.8), respectively. WLI and NBI simultaneously had an accuracy of 90.0% (95% CI: 80.7–99.3), sensitivity of 90.0% (95% CI: 79.3–100.7), and specificity of 90.0% (95% CI: 71.4–108.6),

respectively. WLI and NBI simultaneously resulted in a significantly higher accuracy than WLI alone (P = 0.035), whereas WLI and VICI simultaneously tended to result in a higher accuracy than WLI alone (P = 0.083). However, no significant differences were observed between the accuracies of WLI and NBI or between WLI and VICI (P=0.65). (Fig. 5). The AUCs of WLI alone, WLI and VICI simultaneously, and simultaneous WLI and NBI were 0.683 (95% CI: 0.487–0.831), 0.850 (95% CI: 0.651–0.945), and 0.900 (95% CI: 0.721–0.969), respectively. No significant difference was observed in the AUC between WLI and WLI and VICI simultaneously, or between WLI and NBI simultaneously (P=0.13 and P=0.057, respectively) (Fig. 6).

DISCUSSION

To the best of our knowledge, this is the first report showing the diagnostic utility of VICI in converted POCS images using "CycleGAN." VICI outperformed WLI and NBI in terms of visualization of surface structures and lesion margins. Additionally, the diagnostic accuracy improved using both WLI and VICI compared to using WLI alone. VICI may be used in combination with WLI and NBI for evaluating biliary lesions, not only malignant or benign lesions, but also the extent of the lesions.

In the context of biliary tract lesions, the macroscopic classification of non-neoplastic and neoplastic lesions using CRM and the Mendoza classification has been reported[9]. According to this classification, the sensitivity for detecting neoplastic lesions was 96.3%, with a specificity of 92.3%. Thus, visualization of surface structures is crucial for the accurate diagnosis of biliary tract lesions. Furthermore, cholangiocarcinoma often progresses over the superficial layers of the bile duct mucosa[10]; therefore, evaluating the lesion margin with POCS is important and potentially valuable for achieving a high rate of R0 resection[11,12]. Indigo carmine spraying is beneficial in gastrointestinal endoscopy for evaluating surface structures

and lesion margins. It has proven useful in early gastric cancer diagnosis and detection of dysplastic lesions in inflammatory bowel disease [13]. VICI has already been reported in clinical practice in gastrointestinal endoscopy, and it achieved high similarity with the manifestation after a real spray of indigo carmine[14]. In cases where indigo carmine spraying within the bile duct is challenging, VICI has emerged as an ideal modality. In our study, surface structure and lesion margin visualization received high praise from expert endoscopists, further emphasizing the utility of VICI.

NBI has become an indispensable modality in gastrointestinal endoscopy for the diagnosis of early gastric cancer[15] and colorectal tumors[16]. NBI is also employed in CHF-B260 and CHF-B290 (Olympus Medical, Tokyo, Japan), which facilitates the recognition of microvessels and is applicable in gastrointestinal endoscopy. The presence or absence of irregular microvessels in the bile duct lesions is a crucial discriminator between benign and malignant conditions[17]. NBI has been reported to be useful in predicting malignancy in indeterminate biliary strictures, with an accuracy of 91.3%, compared to 82.8% for WLI[4]. Moreover, reports indicate that focusing on both surface structures and microvessels in bile duct lesions leads to a higher diagnostic accuracy than focusing on either aspect alone[2]. Consequently, by observing the surface structures and lesion margins with VICI and the surface microvessels with NBI, the combined approach has the potential to achieve higher diagnostic accuracy in qualitative diagnosis and lesion extent assessment.

In the field of gastrointestinal endoscopy, artificial intelligence is becoming increasingly prevalent as an aid in the diagnosis of cancers and adenomas[18]. The two most important aspects of gastrointestinal endoscopy and artificial intelligence are the diagnosis of benign or malignant lesions and image-conversion techniques. In the biliopancreatic field, artificial intelligence has been reported to be beneficial for the diagnosis of benign and malignant conditions using POCS images and videos[19,20]. These reports have demonstrated a

diagnostic accuracy that is on par with that of experts. However, few studies report image transformation techniques in the biliopancreatic field. Previously, we successfully achieved VICI transformation in videos[6]. In the future, we believe that using this transformation in real time can further enhance diagnostic accuracy.

This study had several limitations. First, this study had a limited number of cases and a retrospective design primarily based on endoscopic image evaluation. Furthermore, although this study did not conclusively prove its contribution to achieving R0 resection rates for bile duct cancer, we believe that this innovative intervention in the biliary field has the potential to improve future R0 resection rates. A prospective study combining VICI and biopsy is required to evaluate the diagnostic yield and R0 resection rate. Second, acknowledging that the images used in this study were virtual spraying images, representing a simulation rather than real spraying, is important. The use of indigo-sprayed gastrointestinal images as training data may result in images that differ from actual images captured within the bile duct. Proper evaluation of VICI has a learning curve, which is a novel technology. However, as indigo carmine is widely used in gastrointestinal endoscopy, endoscopists are likely to be familiar with indigo-sprayed images. Moreover, it helps visualize surface irregularities indicative of epithelial changes; therefore, it is particularly useful for evaluating bile ducts. Third, in this study, gastrointestinal endoscope training data and cholangioscopy images of the same vendor for which NBI was available were used. Previous studies on artificial intelligence performance in POCS have used SpyGlass™ (Boston Scientific Corp., Natick, MA, USA). Future development of virtual chromoendoscopy artificial intelligence that is not vendor-specific is desired as it would allow for broader applicability beyond a specific vendor's equipment.

In conclusion, VICI for POCS is valuable for visualizing surface structures and lesion margins. Although further prospective multicenter studies evaluating the diagnostic yield of VICI in combination with biopsy are required, VICI may be an essential modality for POCS,

in addition to NBI.

References

1. Fukuda Y, Tsuyuguchi T, Sakai Y, Tsuchiya S, Saisyo H. Diagnostic utility of peroral cholangioscopy for various bile-duct lesions. Gastrointest Endosc. 2005;62(3):374–82. doi: 10.1016/j.gie.2005.04.032.
2. Shin IS, Moon JH, Lee YN, Kim HK, Chung JC, Lee TH, et al. Detection and endoscopic classification of intraductal neoplasms of the bile duct by peroral cholangioscopy with narrow-band imaging (with videos). Gastrointest Endosc. 2023;97(5):898–910. doi: 10.1016/j.gie.2023.01.008.
3. Muto M, Horimatsu T, Ezoe Y, Morita S, Miyamoto S. Improving visualization techniques by narrow band imaging and magnification endoscopy. J Gastroenterol Hepatol. 2009;24(8):1333–46. doi: 10.1111/j.1440-1746.2009.05925.x.
4. Shin IS, Moon JH, Lee YN, Kim HK, Lee TH, Yang JK, et al. Efficacy of narrow-band imaging during peroral cholangioscopy for predicting malignancy of indeterminate biliary strictures (with videos). Gastrointest Endosc. 2022;96(3):512–21. doi: 10.1016/j.gie.2022.04.017.
5. Peitz U, Malfertheiner P. Chromoendoscopy: From a research tool to clinical progress. Dig Dis. 2002;20(2):111–9. doi: 10.1159/000067480.
6. Sato R, Matsumoto K, Kinugasa H, Uchida D, Kato H, Otsuka M, et al. Usefulness of the artificial intelligence-mediated virtual chromoendoscopy in peroral cholangioscopy. Endoscopy. 2023;55(S 01):E971–2. doi: 10.1055/a-2142-4555.
7. Zhu JY, Park T, Isola P, Efros AA. Unpaired image-to-image translation using cycle-consistent adversarial networks IEEE International Conference on Computer Vision, Venice, Italy. 2017; p. 2242–51. doi: 10.1109/ICCV.2017.244.
8. Yamamoto S, Kinugasa H, Hamada K, Tomiya M, Tanimoto T, Ohto A, et al. The diagnostic ability to classify neoplasias occurring in inflammatory bowel disease by

artificial intelligence and endoscopists: A pilot study. J Gastroenterol Hepatol. 2022;37(8):1610–6. doi: 10.1111/jgh.15904.

9. Robles-Medranda C, Valero M, Soria-Alcivar M, Puga-Tejada M, Oleas R, Ospina-Arboleda J, et al. Reliability and accuracy of a novel classification system using peroral cholangioscopy for the diagnosis of bile duct lesions. Endoscopy. 2018;50(11):1059–70. doi: 10.1055/a-0607-2534.

10. Nakanishi Y, Zen Y, Kawakami H, Kubota K, Itoh T, Hirano S, et al. Extrahepatic bile duct carcinoma with extensive intraepithelial spread: a clinicopathological study of 21 cases. Mod Pathol. 2008;21(7):807–16. doi: 10.1038/modpathol.2008.65.

11. Fukasawa Y, Takano S, Fukasawa M, Maekawa S, Kadokura M, Shindo H, et al. Form-Vessel classification of cholangioscopy findings to diagnose biliary tract carcinoma's superficial spread. Int J Mol Sci. 2020;21(9):3311. doi: 10.3390/ijms21093311.

12. Nagakawa Y, Kasuya K, Bunso K, Hosokawa Y, Kuwabara H, Nakagima T, et al. Usefulness of multi-3-dimensional computed tomograms fused with multiplanar reconstruction images and peroral cholangioscopy findings in hilar cholangiocarcinoma. J Hepato-Bil Pancreat Sci. 2014;21(4):256–62. doi: 10.1002/jhbp.85.

13. Singh R, Chiam KH, Leiria F, Pu LZCT, Choi KC, Militz M. Chromoendoscopy: Role in modern endoscopic imaging. Transl Gastroenterol Hepatol. 2020;5:39. doi: 10.21037/tgh.2019.12.06.

14. Yuan X, Gong W, Hu B. Virtual indigo carmine dyeing: new artificial intelligence-based chromoendoscopy technique. Dig Endosc. 2023;35(1):e8–ee10. doi: 10.1111/den.14448.

15. Muto M, Yao K, Kaise M, Kato M, Uedo N, Yagi K, et al. Magnifying endoscopy simple diagnostic algorithm for early gastric cancer (MESDA-G). Dig Endosc. 2016;28(4):379–93. doi: 10.1111/den.12638.

16. Sano Y, Tanaka S, Kudo SE, Saito S, Matsuda T, Wada Y, et al. Narrow-band imaging (NBI) magnifying endoscopic classification of colorectal tumors proposed by the Japan NBI Expert Team. Dig Endosc. 2016;28(5):526–33. doi: 10.1111/den.12644.

17. Robles-Medranda C, Oleas R, Sánchez-Carriel M, Olmos JI, Alcívar-Vásquez J, Puga-Tejada M, et al. Vascularity can distinguish neoplastic from non-neoplastic bile duct lesions during digital single-operator cholangioscopy. Gastrointest Endosc. 2021;93(4):935–41. doi: 10.1016/j.gie.2020.07.025.

18. Okagawa Y, Abe S, Yamada M, Oda I, Saito Y. Artificial intelligence in endoscopy. Dig Dis Sci. 2022;67(5):1553–72. doi: 10.1007/s10620-021-07086-z.

19. Saraiva MM, Ribeiro T, Ferreira JPS, Boas FV, Afonso J, Santos AL, et al. Artificial intelligence for automatic diagnosis of biliary stricture malignancy status in single-operator cholangioscopy: a pilot study. Gastrointest Endosc. 2022;95(2):339–48. doi: 10.1016/j.gie.2021.08.027.

20. Robles-Medranda C, Baquerizo-Burgos J, Alcivar-Vasquez J, Kahaleh M, Raijman I, Kunda R, et al. Artificial intelligence for diagnosing neoplasia on digital cholangioscopy: Development and multicenter validation of a convolutional neural network model. Endoscopy. 2023;55(8):719–27. doi: 10.1055/a-2034-3803.

Figure and Video legends

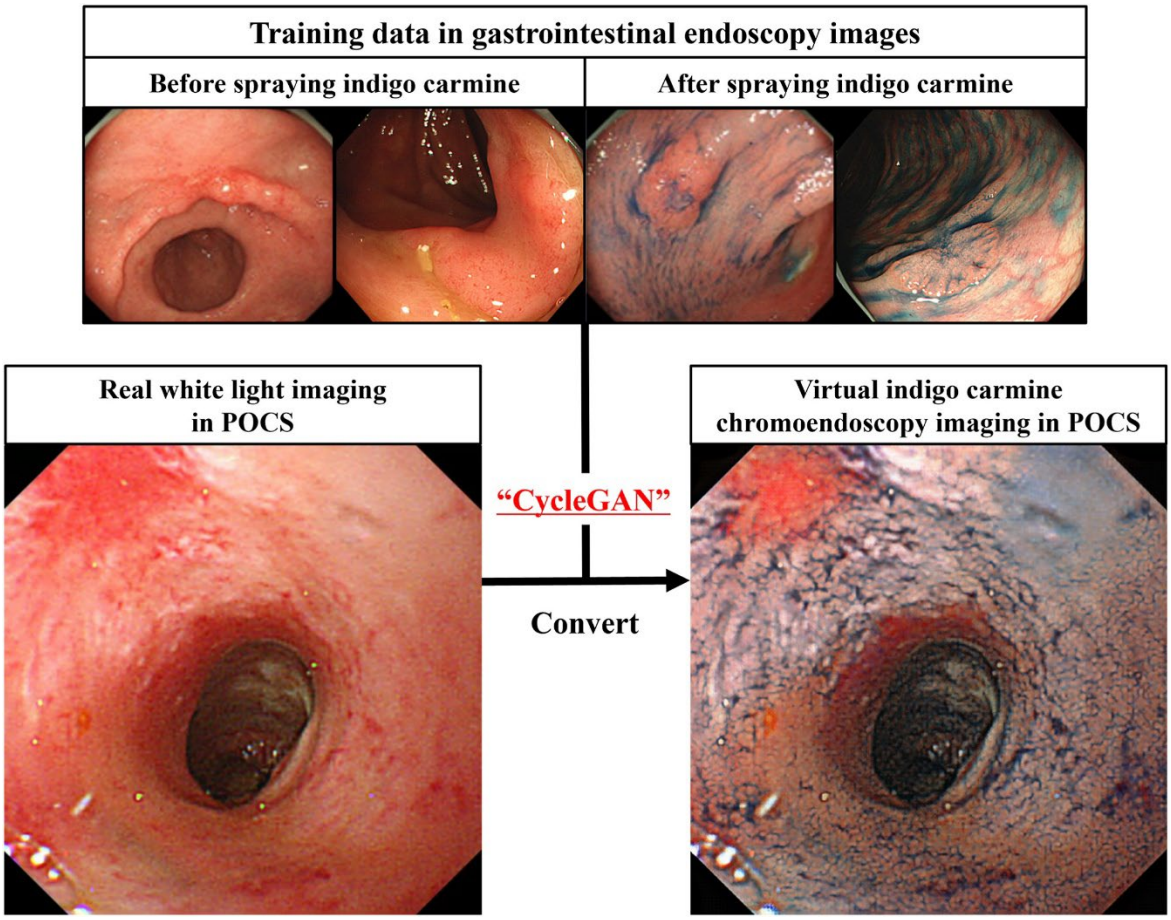

Figure 1. Converting POCS images to virtual indigo carmine chromoendoscopy images using "CycleGAN" by diverting training data in gastrointestinal endoscopy. POCS, peroral cholangioscopy; CycleGAN, cycle-consistent adversarial network

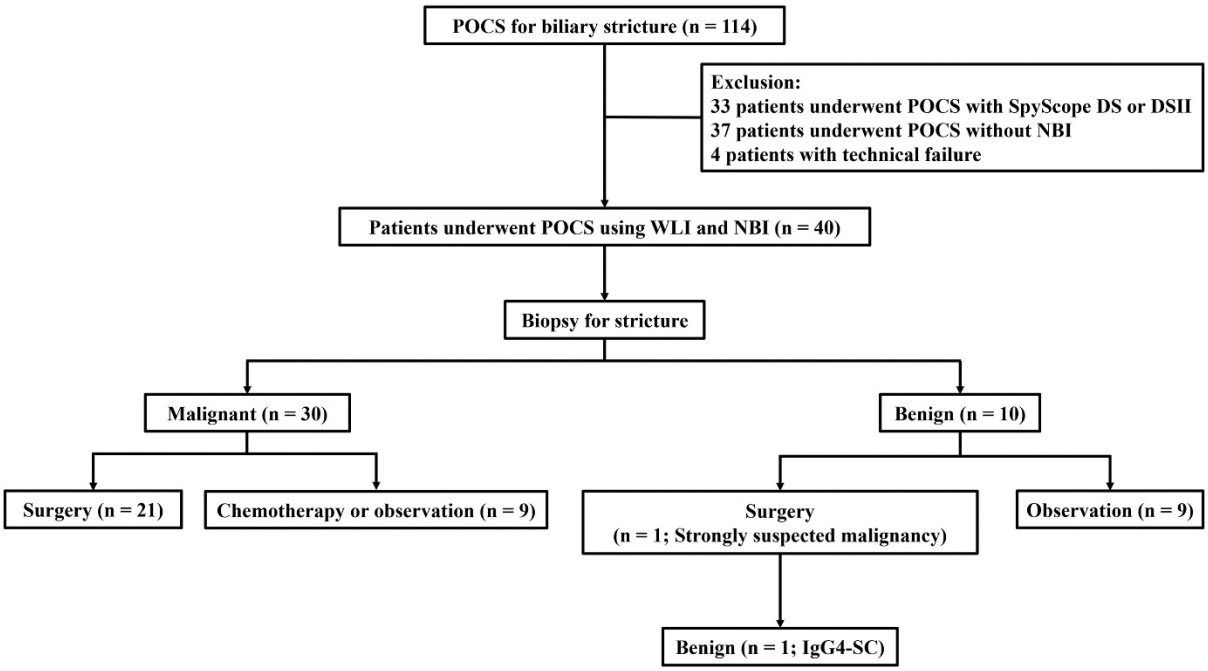

Figure 2. Patient flowchart. POCS, peroral cholangioscopy; NBI, narrow-band imaging; WLI, white light imaging; IgG4-SC, immunoglobulin G4-related sclerosing cholangitis

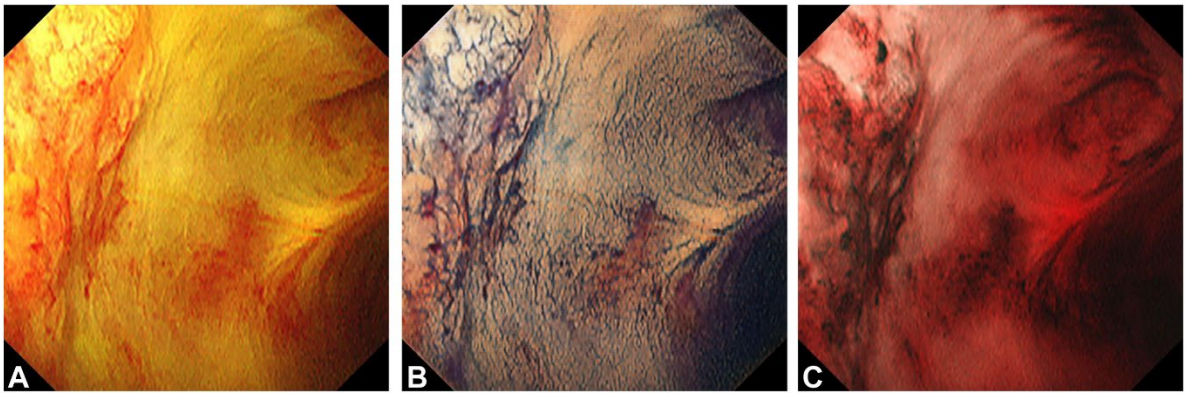

Figure 3. WLI (A), VICI (B), and NBI (C) POCS images of hilar bile duct cancer. VICI visualizes the lesion margin clearly and NBI visualizes the microvessels of the lesion. NBI, narrow-band imaging; POCS, peroral cholangioscopy; VICI, virtual indigo carmine chromoendoscopy; WLI, white light imaging

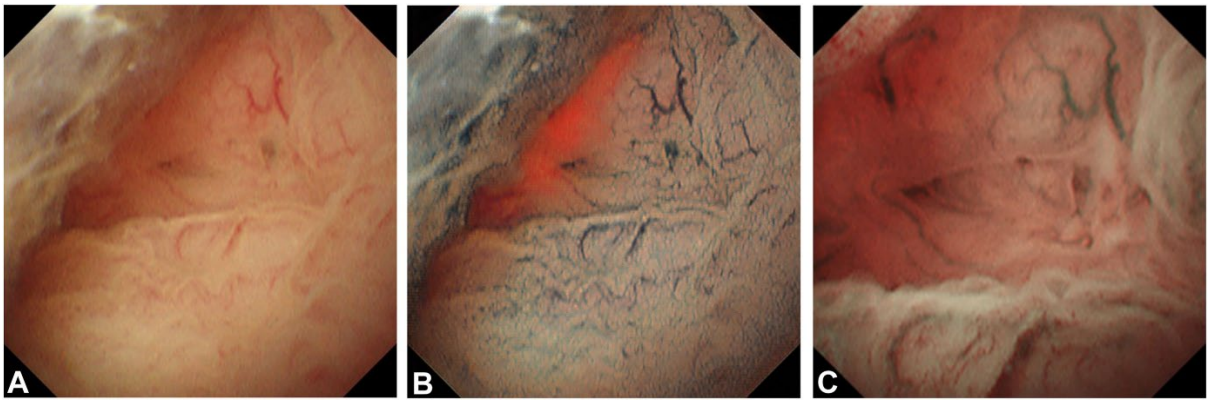

Figure 4. WLI (A), VICI (B), and NBI (C) POCS images of follicular cholangitis. VICI visualizes the surface structures and NBI shows no irregular surface microvessels. NBI, narrow-band imaging; POCS, peroral cholangioscopy; VICI, virtual indigo carmine chromoendoscopy; WLI, white light imaging

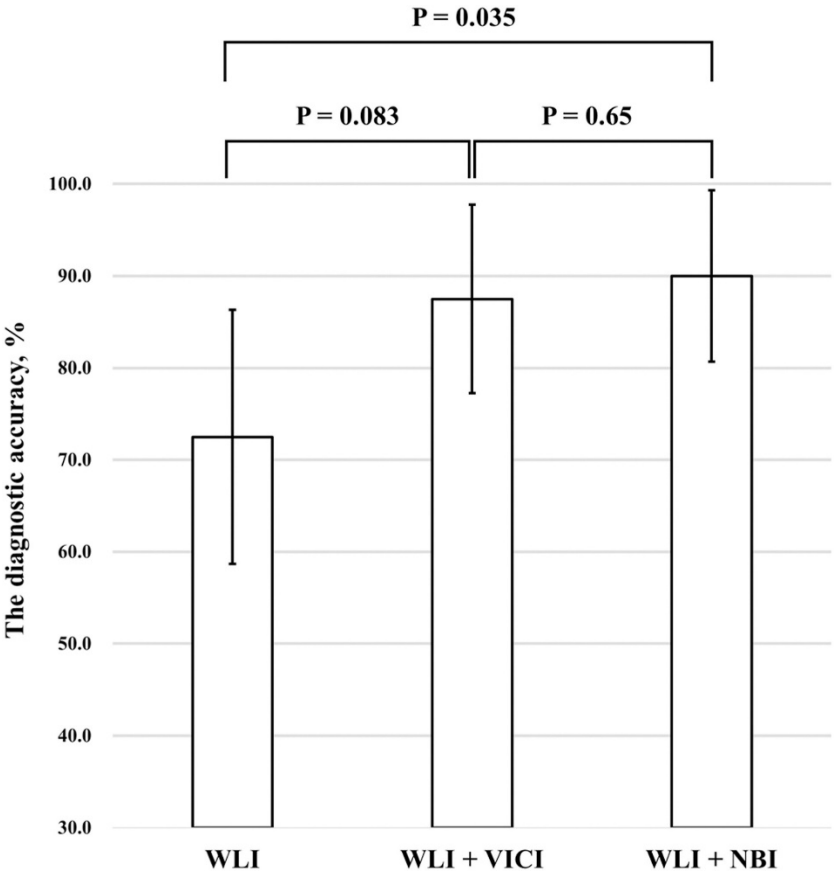

Figure 5. The diagnostic accuracy by endoscopists showing that WLI alone had an accuracy of 72.5%, WLI and VICI simultaneously of 87.5%, and WLI and NBI simultaneously of 90.0%.

WLI and NBI simultaneously resulted in a significantly higher accuracy than WLI alone (P = 0.035), while WLI and VICI simultaneously tended to result in higher accuracy than WLI alone (P = 0.083). No significant difference was observed between the accuracy of WLI and NBI, and WLI and VICI (P = 0.65). NBI, narrow-band imaging; VICI, virtual indigo carmine chromoendoscopy; WLI, white light imaging

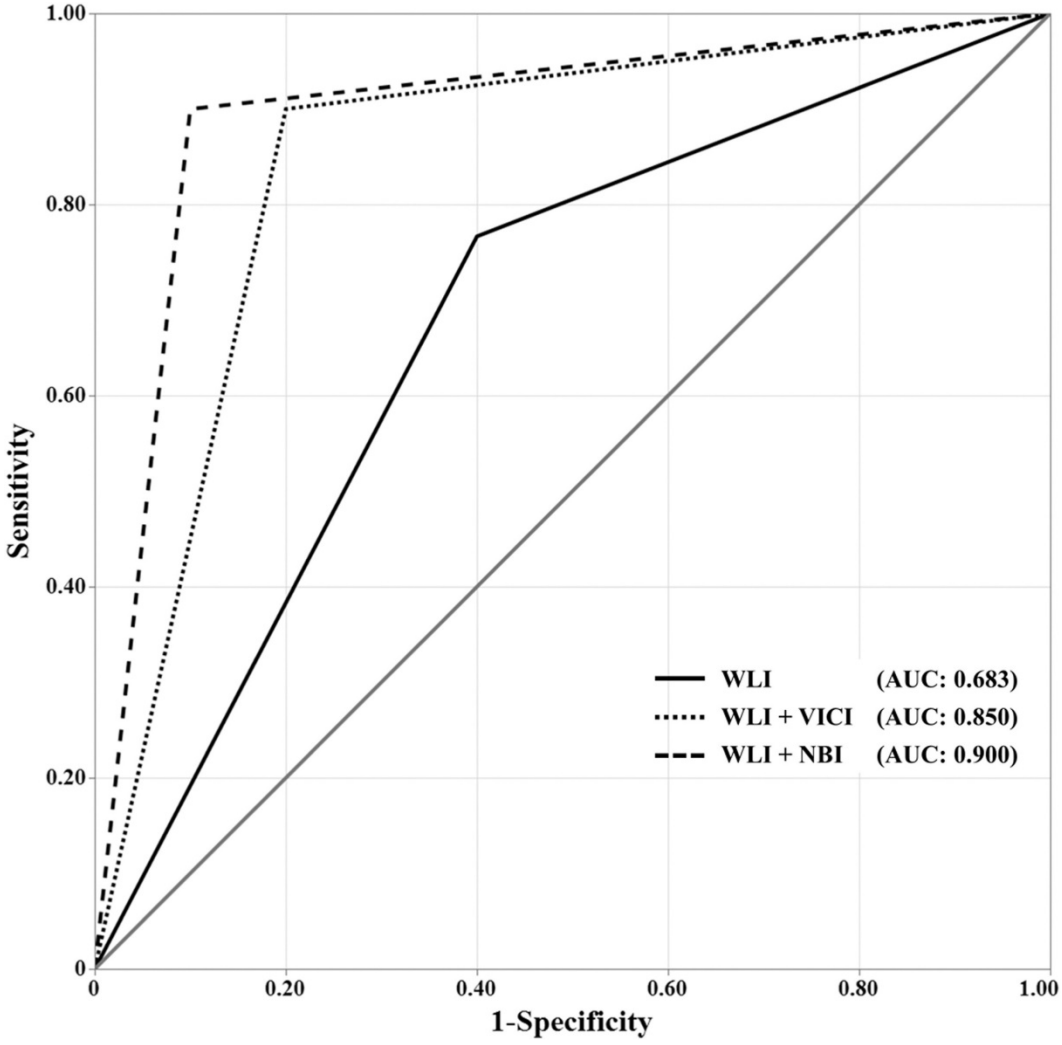

Figure 6. The AUCs of WLI alone, WLI and VICI simultaneously, and WLI and NBI simultaneously were 0.683, 0.850, and 0.900, respectively. AUC, area under the curve; VICI, virtual indigo carmine chromoendoscopy; WLI, white light imaging

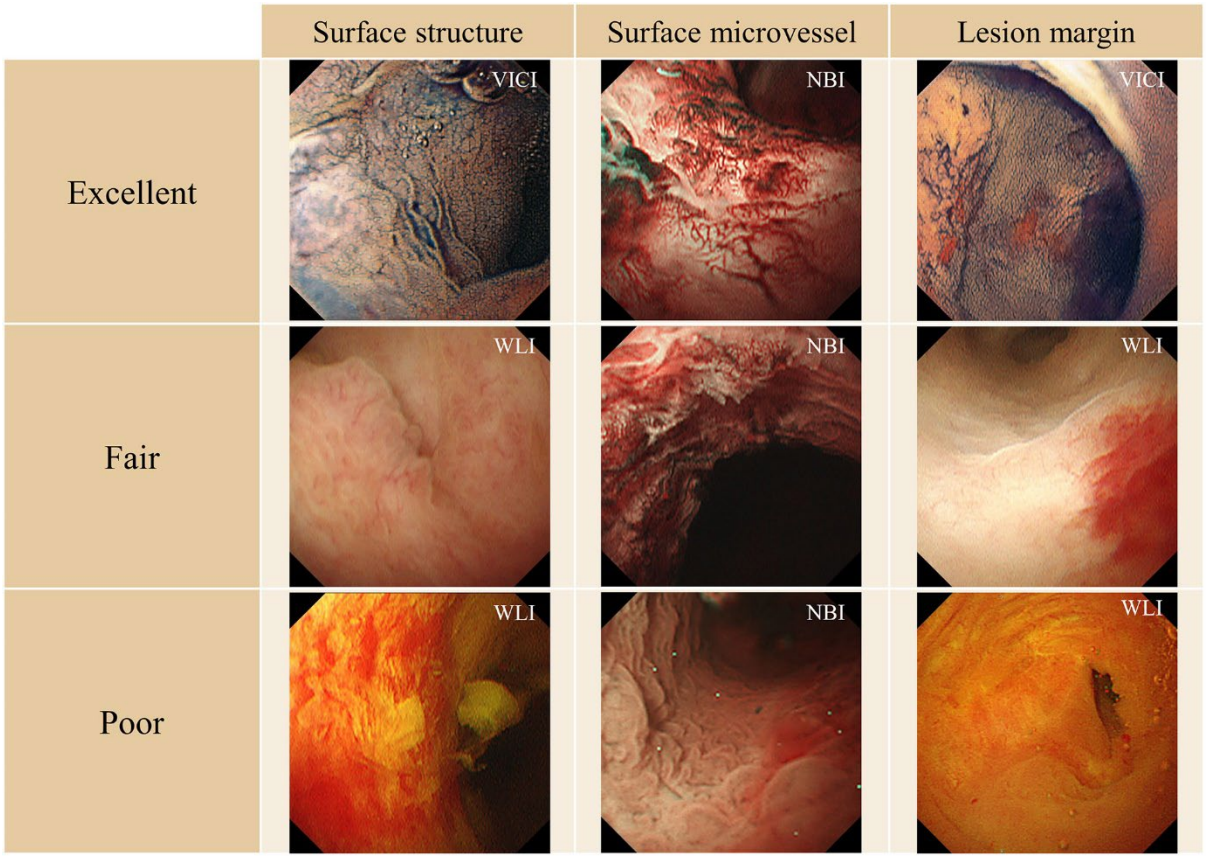

Supplementary Figure 1. Examples of each evaluation for surface structures, surface microvessels, and lesion margins

Video 1. POCS was performed on a patient with hilar bile duct cancer and WLI images were converted to VICI using ”CycleGAN.” POCS, peroral cholangioscopy; WLI, white light imaging; VICI, virtual indigo carmine chromoendoscopy; CycleGAN, cycle-consistent adversarial network

Table 1. Patient characteristics

		n = 40	
Median age, years (range)			74 (47–89)
Sex (Male/Female)			33/7
Symptom, n (%)		Elevated liver enzyme	14 (35.0)
		Jaundice	11 (27.5)
		Abdominal pain	5 (12.5)
		Fever	1 (2.5)
		Asymptomatic	9 (22.5)
Stricture site, n (%)		Hilar	22 (55.0)
		Distal	18 (45.0)
POCS scope, n (%)		CHF-B290	21 (52.5)
		CHF-B260	19 (47.5)
Final diagnosis, n (%)	Malignant		30 (75.0)
		Distal bile duct cancer	15 (37.5)
		Hilar bile duct cancer	12 (30.0)
		Intrahepatic bile duct cancer	2 (5.0)
		Gallbladder cancer	1 (2.5)
	Benign		10 (25.0)
		Secondary sclerosing cholangitis	5 (12.5)
		IgG4-SC	3 (7.5)
		Anastomotic stricture after LDLT	1 (2.5)
		Follicular cholangitis	1 (2.5)

POCS, peroral cholangioscopy; IgG4-SC, immunoglobulin G4-related sclerosing cholangitis

LDLT, living donor liver transplantation

Table 2. Comparison of endoscopic visualization using WLI, VICI, and NBI for biliary strictures

	Poor	Fair	Excellent	P-value	P-value	
	Surface structure, n			Friedman test	Steel-Dwass test	
WLI	6	27	7		< 0.001	(WLI vs VICI)
VICI	3	8	29	< 0.001	< 0.001	(VICI vs NBI)
NBI	9	27	4		0.47	(NBI vs WLI)
	Surface microvessel, n					
WLI	8	25	7		< 0.001	(WLI vs VICI)
VICI	33	7	0	< 0.001	< 0.001	(VICI vs NBI)
NBI	4	8	28		< 0.001	(NBI vs WLI)
	Lesion margin, n					
WLI	2	34	4		0.004	(WLI vs VICI)
VICI	4	15	21	< 0.001	< 0.001	(VICI vs NBI)
NBI	12	22	6		0.21	(NBI vs WLI)

WLI, white light imaging; VICI, virtual indigo carmine chromoendoscopy; NBI, narrow-band imaging

Supplementary Table 1. Grading of 10 VICI sample images in POCS by three endoscopists

	Image 1	Image 2	Image 3	Image 4	Image 5	Image 6	Image 7	Image 8	Image 9	Image 10
					Surface structures					
Endoscopist A	Fair	Excellent	Fair	Excellent	Excellent	Excellent	Excellent	Excellent	Fair	Excellent
Endoscopist B	Excellent	Fair	Excellent	Excellent	Excellent	Excellent	Fair	Excellent	Excellent	Excellent
Endoscopist C	Excellent	Excellent	Excellent	Excellent	Fair	Excellent	Poor	Excellent	Excellent	Fair
					Surface microvessels					
Endoscopist A	Poor	Poor	Poor	Poor	Poor	Poor	Fair	Poor	Poor	Poor
Endoscopist B	Poor	Poor	Poor	Poor	Fair	Poor	Poor	Poor	Poor	Poor
Endoscopist C	Poor	Fair	Poor	Poor	Poor	Poor	Poor	Poor	Fair	Fair
					Lesion margins					
Endoscopist A	Excellent	Excellent	Excellent	Fair	Excellent	Fair	Excellent	Fair	Excellent	Fair
Endoscopist B	Fair	Fair	Excellent	Fair	Excellent	Excellent	Poor	Excellent	Fair	Excellent
Endoscopist C	Poor	Excellent	Fair	Excellent	Fair	Fair	Fair	Excellent	Excellent	Poor